

# Magnitude and Nature of Interactions in Benzene–X (X = Ethylene and Acetylene) in the Gas Phase: Significantly Different CH/ $\pi$ Interaction of Acetylene As Compared with Those of Ethylene and Methane

Kenta Shibasaki,<sup>†</sup> Asuka Fujii,<sup>\*,‡</sup> Naohiko Mikami,<sup>†</sup> and Seiji Tsuzuki<sup>\*,‡</sup>

Department of Chemistry, Graduate School of Science, Tohoku University, Sendai 980-8578, Japan, and National Institute of Advanced Industrial Science and Technology (AIST), Tsukuba, Ibaraki 305-8568, Japan

Received: August 7, 2006; In Final Form: December 6, 2006

The accurate interaction energies of the CH/ $\pi$  interaction in the benzene–X clusters (X = ethylene and acetylene) were experimentally and theoretically determined. Two-color multiphoton ionization spectroscopy was applied, and the binding energies in the neutral ground state of the clusters were evaluated from the dissociation threshold measurements of the cluster cations. The experimental binding energies of the clusters ( $D_0$ ) were  $1.4 \pm 0.2$  and  $2.7 \pm 0.2$  kcal/mol, respectively. Estimated CCSD(T) interaction energies for the clusters at the basis set limit ( $D_e$ ) were 2.2 and 2.8 kcal/mol, respectively. Calculated  $D_0$  values (1.7 and 2.4 kcal/mol, respectively) are close to the experimental values. Large electron correlation contributions ( $E_{\text{corr}} = -3.6$  and  $-2.8$  kcal/mol, respectively) show that dispersion is the major source of the attraction in both clusters. The electrostatic interaction in the ethylene cluster is very small ( $-0.38$  kcal/mol), as in the case of the benzene–methane cluster, whereas the electrostatic interaction in the acetylene cluster is large ( $-1.70$  kcal/mol). The shifts of the  $S_1$ – $S_0$  transition also suggest that the ethylene cluster is a van der Waals-type cluster, but the acetylene cluster is a  $\pi$ –hydrogen-bonded cluster. The nature of the CH/ $\pi$  interaction of the “activated” alkyne C–H bond is significantly different from that of the “nonactivated” (or typical) alkane and alkene C–H bonds.

## Introduction

The magnitude of an intermolecular interaction energy is the most fundamental physical quantity to study the intermolecular interaction. For many weak and unconventional intermolecular interactions, however, reliable experimental data have not yet been reported, and only theoretical estimations are available.<sup>1–3</sup> Although recent high-level quantum chemical calculations are highly accurate in energy estimation, comparison with experimental results is still strongly desired, especially for weak intermolecular interactions to confirm their accuracy.

To determine accurate intermolecular interaction energies, isolated binary clusters in the gas phase are ideal systems, especially for weak interactions.<sup>4,5</sup> In the gas-phase clusters, competing interactions in the bulk phase are totally eliminated, and various fine spectroscopic techniques are applicable for the energy determination. Moreover, experimental values in the gas-phase clusters can be directly compared with theoretical estimations.

The CH/ $\pi$  interaction is an attractive force between a C–H bond and a  $\pi$  electron system, and the role of this interaction in various molecular functions, such as molecular recognitions and crystal packing, has been discussed.<sup>1,3,6,7</sup> The CH/ $\pi$  interaction is a weak intermolecular interaction, and its magnitude is believed to lie in the gray region between the weakest class of hydrogen bond and the dispersion interaction.

The nature of the C–H/ $\pi$  interaction is not uniform, but changes from the van der Waals type to the  $\pi$ –hydrogen-bond-

like nature, depending on the acidity of the C–H bond. The acidity of alkyne is higher than that of alkene and alkane (the pKa value of acetylene is 25; those of ethylene and methane are 45 and 59, respectively).<sup>8</sup> The interaction between a C–H bond of alkyne and  $\pi$  electrons is strongly enhanced in comparison with that of the “typical” C–H/ $\pi$  interaction of a C–H bond of alkane, and it is often called “activated” C–H/ $\pi$  interaction.<sup>3,9–12</sup> High solubility of acetylene in benzene has been well-known,<sup>13,14</sup> and it has been attributed to the “activated” C–H/ $\pi$  interaction. Remarkable low-frequency shifts of the C–H stretching vibration are also observed for acetylene solved in bulk benzene and an acetylene–benzene mixture in an Ar matrix.<sup>15–17</sup> Such a spectral feature in the benzene–acetylene system has been extensively examined in gas-phase IR studies of the binary clusters, and the cluster structure, where the acetylenic C–H bond directly interacts with the  $\pi$ –electrons of benzene, has been confirmed.<sup>12,18</sup> The remarkable low-frequency shifts of the C–H stretch frequency in the benzene–acetylene system suggest the  $\pi$ –hydrogen bond character of the “activated” CH/ $\pi$  interaction. The binary cluster study by Fujii et al. showed that the magnitude of the acetylenic C–H frequency shift depends on the  $\pi$ –electron density of the aromatic ring.<sup>12</sup> On the other hand, the C–H frequency shift is very small in the benzene–methane cluster.<sup>19</sup> Ab initio calculations show that the contribution of the electrostatic term is as large as that of the dispersion term in benzene–acetylene, whereas the dispersion interaction is dominant in benzene–methane.<sup>10</sup> Although the pKa value of ethylene is substantially larger than that of acetylene, the difference between the CH/ $\pi$  interaction of ethylene and that of acetylene has not yet been clearly understood.

\* Corresponding authors. E-mails: (A.F.) asukafujii@mail.tains.tohoku.ac.jp, (S.T.) s.tsuzuki@aist.go.jp.

<sup>†</sup> Tohoku University.

<sup>‡</sup> AIST.

High-level ab initio calculations predicted that the magnitude of the interaction energies with benzene increases in the order of methane, ethylene, and acetylene.<sup>10</sup> In the previous paper, we applied mass-analyzed threshold ionization (MATI) spectroscopy to the benzene–methane cluster in the gas phase, which can be regarded as a prototype system for the CH/ $\pi$  interaction between a C–H bond and  $\pi$  electrons, and determined the accurate interaction energy to be 1.03–1.13 kcal/mol.<sup>20</sup> However, experimental measurements of the binding energies of the benzene clusters with acetylene and ethylene have not yet been reported.

In the present paper, the C–H/ $\pi$  interaction energies in the benzene–ethylene and benzene–acetylene clusters (the binding energies of these clusters in the neutral ground state) are experimentally and theoretically determined. In our previous study, the interaction energy in benzene–methane was precisely measured by MATI spectroscopy.<sup>20</sup> The benzene–ethylene and benzene–acetylene clusters, however, show large structural changes upon ionization, and it makes it difficult to apply the MATI technique to these systems because the Franck–Condon distribution is extensively scattered into the intermolecular vibrational levels. Then, we employ a simple mass-selected, two-color, multiphoton ionization technique to determine the dissociation threshold of the cluster cations. The binding energies of the clusters in the *neutral* ground state (C–H/ $\pi$  interaction energies) are evaluated by the relation between the dissociation energy in the cationic state and the ionization potential. The experimentally determined interaction energies are compared to estimated CCSD(T) interaction energies at the basis set limit. Although the estimated CCSD(T) interaction energies for the benzene–acetylene and benzene–ethylene clusters were reported, geometries of the two clusters were not optimized.<sup>10</sup> In this study, we fully optimize the geometries and calculate vibrational frequencies for evaluating the effects of zero-point vibrations on the binding energies. In addition, more improved basis sets are used for an accurate estimation of the CCSD(T) interaction energies at the basis set limit. The origin of the enhanced magnitude of the “activated” C–H/ $\pi$  interaction is discussed on the basis of the theoretical calculations supported by the experimental measurements.

## Experimental Section

The dissociation energies of the benzene–ethylene and benzene–acetylene clusters in the cationic state were measured by the mass-selected two-color multiphoton ionization under the molecular beam condition. Details of the experimental setup have been described elsewhere, and only brief descriptions are given here.<sup>20</sup>

Clusters prepared in the molecular beam were pumped to the  $S_1$  vibronic level by the first pulsed laser light ( $\nu_1$ ), the wavelength of which was fixed to be resonant on the  $S_1$ – $S_0$  vibronic band of the cluster. The cluster was successively ionized by the second pulsed laser light ( $\nu_2$ ). Produced ions were mass-selected by a Wiley–McLaren-type time-of-flight (TOF) mass spectrometer,<sup>21</sup> and were detected by a multichannel plate detector. By monitoring the parent cluster ion and fragment ion (benzene monomer cation) intensities, the  $\nu_2$  wavelength was scanned over the dissociation threshold of the cluster cation. The dissociation threshold of the cluster is shown by the rise of the fragment ion signal along the excess ionization energy. The binding energy of the cluster in the neutral ground state was evaluated by the relation among the dissociation energies in the neutral and cationic clusters and the ionization potential of the benzene monomer molecule.

The stationary electric fields were used for the extraction and acceleration of the produced ions into the TOF mass spectrometer. It has been known that field ionization of high Rydberg states decreases the effective ionization threshold energy.<sup>22,23</sup> In the present measurements, the field ionization of the Rydberg cluster and Rydberg fragment also causes the same effect. It has been well-established that the magnitude of the low-frequency shift of the threshold  $\Delta E$  ( $\text{cm}^{-1}$ ) is given by

$$\Delta E \cong 6\sqrt{F} \quad (1)$$

where  $F$  is the magnitude of the static electric field (V/cm) for the ion extraction.<sup>22,23</sup> We employed the ion extraction field of 100 and 500 V/cm for the benzene–ethylene and benzene–acetylene experiments, respectively. The resultant low-frequency shifts of the observed threshold are evaluated to be  $60 \pm 10$  and  $135 \pm 20 \text{ cm}^{-1}$ , respectively. The uncertainties of these field correction terms are due to the slightly non-uniform electric field, which comes from the limited size of the ion extraction electrode and the nearby neutral skimmer.

The benzene sample was purchased from Tokyo Kasei Co. and was used without further purification. The benzene vapor was seeded in a neon–ethylene (or –acetylene) gaseous mixture with a total stagnation pressure at 2–4 atm. The ethylene (acetylene) concentration was adjusted to be 15–20%, and the vapor pressure of the benzene sample was controlled by the sample reservoir temperature for the optimization of the cluster signal intensity.

## Theoretical Calculations

The Gaussian 03 program<sup>24</sup> was used for ab initio calculations of intermolecular interaction energies in the benzene–ethylene and benzene–acetylene clusters. The basis sets implemented in the program were used. Electron correlation was accounted for at the MP2 (second-order Møller–Plesset perturbation)<sup>25,26</sup> and CCSD(T) (coupled cluster calculations with single and double substitutions with noniterative triple excitations) levels.<sup>27</sup> Geometries of the clusters were optimized at the MP2/cc-pVTZ level. Vibrational frequencies were calculated at the same level. Accuracy of the optimized geometries is discussed in the Supporting Information. Basis set superposition error (BSSE) was corrected for all calculations with the counterpoise method.<sup>28,29</sup> The MP2 level interaction energy at the basis set limit [ $E_{\text{MP2}(\text{limit})}$ ] was estimated by Helgaker’s method from calculated MP2 interaction energies ( $E_{\text{MP2}}$ ) using aug-cc-pVTZ and aug-cc-pVQZ basis sets.<sup>30</sup> In Helgaker’s method, the  $E_{\text{MP2}}$  calculated with Dunning’s correlation consistent basis sets were fitted to a form  $a + bX^{-3}$  (where  $X$  is 3 for aug-cc-pVTZ and 4 for aug-cc-pVQZ). The  $E_{\text{MP2}(\text{limit})}$  was then estimated by extrapolation. Helgaker’s method was originally proposed for an estimation of electron correlation contribution at the basis set limit, but we used this method for an estimation of  $E_{\text{MP2}(\text{limit})}$ , since the two basis sets provided nearly the same HF level interaction energies. Performance of bond functions proposed by Tao and Pan<sup>31</sup> is also discussed in the Supporting Information. The CCSD(T) level interaction energy at the basis set limit [ $E_{\text{CCSD(T)}(\text{limit})}$ ] was calculated as the sum of the  $E_{\text{MP2}(\text{limit})}$  and the estimated CCSD(T) correction term [ $\Delta\text{CCSD(T)} = E_{\text{CCSD(T)}} - E_{\text{MP2}}$ ] at the basis set limit [ $\Delta\text{CCSD(T)}(\text{limit})$ ], which was estimated from the difference between the calculated CCSD(T) and MP2 level interaction energies using the aug-cc-pVDZ basis set.<sup>10</sup> A detailed estimation procedure of the  $\Delta\text{CCSD(T)}(\text{limit})$  is shown in the Supporting Information. Expected errors of the estimated  $E_{\text{CCSD(T)}(\text{limit})}$  are also discussed in the Support-

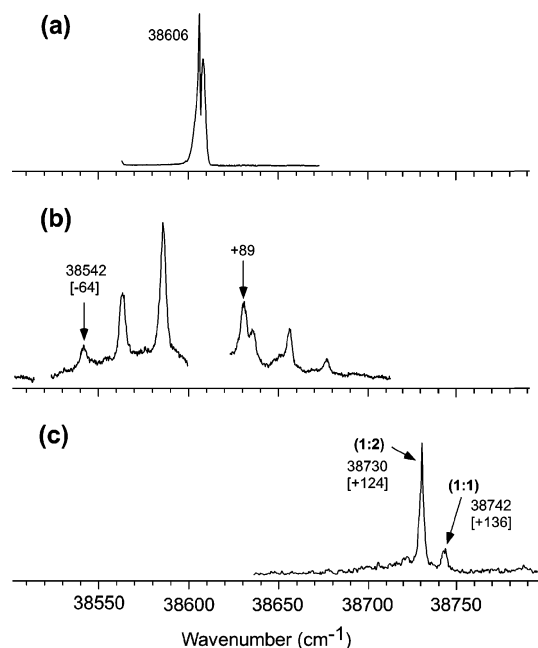


**Figure 1.** One-color, mass-selected, multiphoton ionization spectra of (a) bare benzene, (b) benzene-ethylene, and (c) benzene-acetylene in the  $S_1-S_0$   $6^1_0$  region. The spectra were obtained by monitoring the bare benzene $^+$ , (benzene-ethylene) $^+$ , and (benzene-acetylene) $^+$  cations, respectively. Numbers in the parentheses are relative frequencies from the  $6^1_0$  band of bare benzene (38 606  $\text{cm}^{-1}$ ).

ing Information. Electrostatic energy was calculated using the Orient program, version 3.2.<sup>32</sup> The electrostatic energy for a cluster was obtained from the interactions between distributed multipoles of monomers.<sup>33,34</sup> Distributed multipoles up to hexadecapole on all atoms were obtained from the MP2/cc-pVTZ wave functions of an isolated molecule using the GDMA program.<sup>35</sup> Distributed multipoles were used only to estimate the electrostatic energy.

## Results and Discussion

**1.  $S_1-S_0$  Electronic Spectra.** Figure 1 shows the mass-selected, one-color, multiphoton ionization (MPI) spectra of (a) bare benzene, (b) benzene-ethylene, and (c) benzene-acetylene in the  $S_1-S_0$   $6^1_0$  region. To measure these spectra, bare benzene $^+$ , (benzene-ethylene) $^+$ , and (benzene-acetylene) $^+$  cations were detected separately. A part of the spectrum of benzene-ethylene is missing because of the interference by the much stronger ion signal due to the transition of bare benzene.

The  $6^1_0$  band of the benzene-ethylene cluster appears at 38542  $\text{cm}^{-1}$ , and it is low-frequency-shifted by 64  $\text{cm}^{-1}$  from the corresponding band of bare benzene. The  $6^1_0$  band of benzene-ethylene is accompanied by a long progression of the combination bands with an intermolecular vibrational mode, which has a harmonic frequency of 23  $\text{cm}^{-1}$ . This would be a bending or torsional motion of the cluster, and the long progression indicates a rearrangement of the cluster structure along this coordinate in the  $S_1$  state.

The  $S_1-S_0$  electronic spectrum of benzene-acetylene has been extensively studied so far.<sup>36-38</sup> In the one-color, multiphoton ionization, most of the cluster cations dissociate upon the ionization, and one acetylene molecule evaporates. Then, the stronger band at 38730  $\text{cm}^{-1}$  in the spectrum (c) is attributed to the 1:2 cluster, and the weaker band at 38742  $\text{cm}^{-1}$  is assigned to the 1:1 cluster. Both of the cluster bands are high-frequency-shifted by 124 and 136  $\text{cm}^{-1}$ , respectively, from the corresponding band of bare benzene.

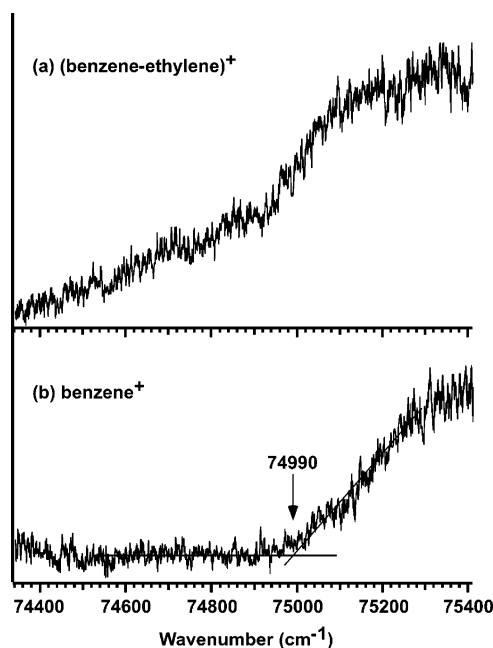


**Figure 2.** Mass-selected, two-color, multiphoton ionization spectra of benzene-ethylene via the combination band at 38 631  $\text{cm}^{-1}$  (+89  $\text{cm}^{-1}$  from the  $S_1-S_0$   $6^1_0$  band; see text). (a) Parent (benzene-ethylene) $^+$  and (b) fragment benzene $^+$  cations were detected to measure the spectra, respectively. The arrow in the figure shows the observed dissociation threshold of the cluster cation.

In aromatic clusters of the van der Waals type, such as benzene-rare gas atom and benzene-tetrachloromethane clusters, the  $S_1-S_0$  electronic transition localized in the aromatic moiety is generally low-frequency-shifted in comparison with that of the bare molecule.<sup>39,40</sup> The low-frequency shift means an enhancement of the binding (interaction) energy of the cluster upon the electronic excitation, and it is caused by the larger polarizability of the aromatic moiety in the electronic excited state. On the other hand, a high-frequency shift is generally seen in  $\pi$ -hydrogen-bonded clusters such as benzene-water.<sup>41</sup> The high-frequency shift means a decrease of the binding energy in the electronic excited state. For the electronic excitation localized in the aromatic moiety, however, the enhancement of the dispersion interaction is expected also in the  $\pi$ -hydrogen-bonded clusters. Therefore, it indicates that the contribution of the electrostatic interaction is more important in the  $\pi$ -hydrogen-bonded clusters, and the reduction of the electrostatic interaction upon the electronic excitation is dominant over the enhancement of the dispersion interaction. The low-frequency shift of the benzene-ethylene cluster suggests that the dispersion force is still dominant in this cluster, being similar to the case of benzene-methane. This is in contrast with the benzene-acetylene cluster, which shows the high-frequency shift in the  $S_1-S_0$  transition. It reflects the remarkable enhancement of the electrostatic interaction in the total intermolecular interactions of benzene-acetylene.

## 2. Experimental Determination of the Binding Energies.

Figure 2 shows the two-color MPI spectra of benzene-ethylene. In these spectra, the  $\nu_1$  laser wavelength was fixed at the vibronic band at 38631  $\text{cm}^{-1}$  (+89  $\text{cm}^{-1}$  from the  $6^1_0$  band), and the  $\nu_2$  laser wavelength was scanned across the dissociation threshold of the cluster cation. The abscissa of the spectra is plotted by the total excitation energy ( $\nu_1 + \nu_2$ ). In the spectra, (a) parent (benzene-ethylene) $^+$  and (b) fragment benzene $^+$  cations were monitored. The vibronic band at 38631  $\text{cm}^{-1}$  was chosen as

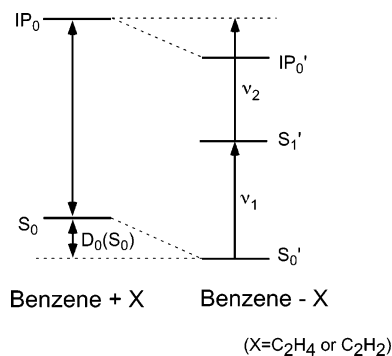


**Figure 3.** Energy scheme to determine the binding energy of the neutral cluster in the  $S_0$  state ( $D_0(S_0)$ ) (see text).

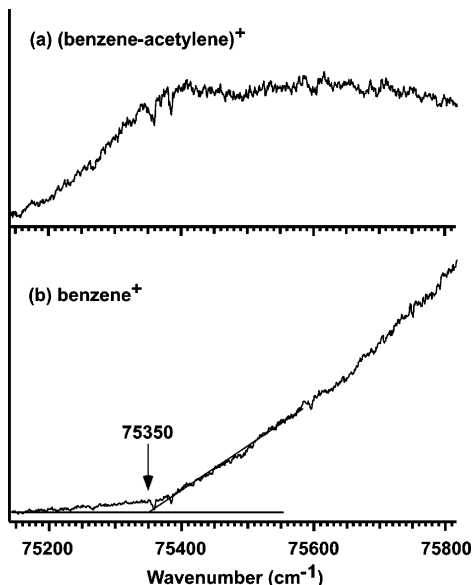


**Figure 4.** Mass-selected, two-color, multiphoton ionization spectra of benzene–acetylene via the  $S_1$ – $S_0$   $6^1_0$  band (see text). (a) Parent (benzene–acetylene)<sup>+</sup> and (b) fragment benzene<sup>+</sup> cations were detected to measure the spectra. The arrow in the figure shows the observed dissociation threshold of the cluster cation.

the first excitation step to avoid interference from the nearby transitions of bare benzene and higher clusters of benzene–ethylene.

Spectrum “a” shows the threshold of the two-color ionization around  $74400\text{ cm}^{-1}$  in the total energy. However, because of the large structural difference of the cluster between the  $S_1$  and cationic states, this would not be an indication of the adiabatic ionization potential. It is reasonable to consider that the rise of the two-color ionization shows the vertical ionization energy. No clear step structure corresponding to a vibrational level of the cluster cation is seen in the spectrum, but the spectrum shows a smooth slope structure, which is an ensemble of unresolved fine step-structures due to the intermolecular vibrations.

When the total excitation energy of the cluster is beyond the dissociation threshold of the cluster cation, the resulting ion of the two-color ionization becomes the benzene<sup>+</sup> fragment. Then, in the two-color MPI spectrum by monitoring the benzene<sup>+</sup> fragment ion (spectrum “b”), a rise is expected at the dissociation threshold. The other spectral sign of the dissociation threshold is a plateau above the threshold in the spectrum by monitoring the parent cluster cation (spectrum “a”). The latter sign occurs because all the increase of the Franck–Condon allowed region with the total excitation energy only contributes to the fragment channel above the dissociation threshold.

Although both of the spectral signs of the threshold should appear at the same excitation energy, the observed spectra of benzene–ethylene show a small displacement of the rise of the fragment cation and beginning of the plateau of the parent cation. When the dissociation lifetime of the cluster cation just above the threshold is long, it makes the threshold unclear because the cluster ions, which survive the ion extraction region, contribute to the parent ion channel intensity. Therefore, it is reasonable to rely on the rise of the fragment ion intensity in spectrum “b” to determine the dissociation threshold. Then, we have the dissociation threshold of (benzene–ethylene)<sup>+</sup> in the range of  $74\,990 \pm 50\text{ cm}^{-1}$ .

The energy scheme of the dissociation energy of the cluster cation and the binding energy in the neutral ground state measured from the zero-point vibrational level ( $D_0(S_0)$ ) is shown in Figure 3. As seen in Figure 3, we have the relation between the total excitation energy at the dissociation threshold of the cluster cation ( $\nu_1 + \nu_2$ ) and the binding energy of the neutral clusters,

$$IP_0 + D_0(S_0) = \nu_1 + \nu_2 \quad (2)$$

where  $IP_0$  is the adiabatic ionization potential of the benzene monomer ( $74\,556\text{ cm}^{-1}$ ).<sup>23</sup> In the analysis of the observed spectra, we need to add the field ionization correction term (1) as follows:

$$IP_0 + D_0(S_0) = \nu_1 + \nu_2 + \Delta E \quad (3)$$

From the observed value of  $\nu_1 + \nu_2$  at the dissociation threshold ( $74\,990 \pm 50\text{ cm}^{-1}$ ) and the field ionization correction ( $60 \pm 10\text{ cm}^{-1}$ ), we evaluate the binding energy of the cluster in the neutral ground state,  $D_0(S_0) = 490 \pm 60\text{ cm}^{-1}$  ( $= 1.4 \pm 0.2\text{ kcal/mol}$ ). This value shows a slight enhancement of the interaction energy in benzene–ethylene in comparison with that in benzene–methane ( $1.03$ – $1.13\text{ kcal/mol}$ ).<sup>20</sup>

We also carried out a similar measurement for the benzene–acetylene cluster. Figure 4 shows the two-color MPI spectra of benzene–acetylene (1:1) via the  $S_1$   $6^1_0$  level by monitoring (a) parent (benzene–acetylene)<sup>+</sup> and (b) fragment benzene<sup>+</sup> cations. In the benzene–acetylene clusters, the rise of the fragment ion signal and the beginning of the plateau of the parent ion signal coincide well with each other at  $75\,350 \pm 40\text{ cm}^{-1}$ . The field ionization correction is  $135 \pm 20\text{ cm}^{-1}$  in this measurement. Thus, the binding energy in the neutral ground state is evaluated to be  $D_0(S_0) = 930 \pm 60\text{ cm}^{-1}$  ( $= 2.7 \pm 0.2\text{ kcal/mol}$ ). This binding energy is twice as large as that in benzene–methane, and it clearly demonstrates the remarkable enhancement of the CH/ $\pi$  interaction of alkyne.

**3. Theoretical Calculations of the Interaction Energies and Comparison with Experimental Results.** Calculated intermolecular interaction energies for the benzene–ethylene and benzene–acetylene clusters (Figure 5) are summarized in Table 1. The basis set dependence of HF interaction energy is negligible, whereas MP2 interaction energy depends strongly on the basis set, as in the case of the benzene–methane cluster. The significant basis set dependence of the MP2 interaction energy shows that an estimation of the  $E_{MP2(\text{limit})}$  is necessary for quantitative evaluation of the interaction energy. The estimated  $E_{MP2(\text{limit})}$  values of the benzene–ethylene and benzene–acetylene clusters are  $-2.82$  and  $-3.50\text{ kcal/mol}$ , respectively. An augmentation of the bond functions proposed by Tao and Pan does not largely change the calculated interaction energy, if large aug-cc-pVTZ and aug-cc-pVQZ basis sets are used.

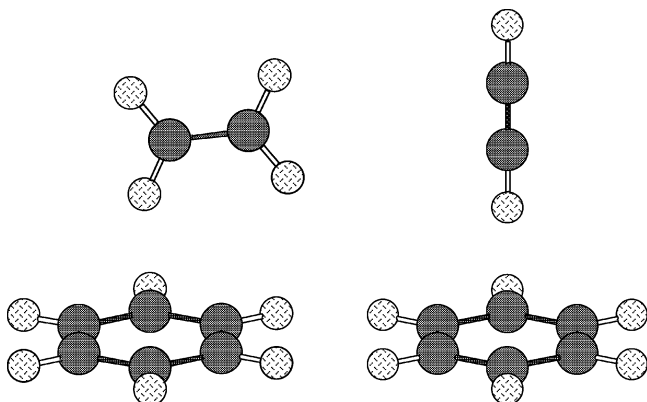


**Figure 5.** Optimized structures of benzene-ethylene and benzene-acetylene clusters at the MP2/cc-pVTZ level.

**TABLE 1: Calculated MP2 and CCSD(T) Interaction Energies for the Benzene-Ethylene and Benzene-Acetylene Clusters<sup>a</sup>**

method	C <sub>6</sub> H <sub>6</sub> -C <sub>2</sub> H <sub>4</sub>	C <sub>6</sub> H <sub>6</sub> -C <sub>2</sub> H <sub>2</sub>
HF/aug-cc-pVDZ	1.401	-0.072
HF/aug-cc-pVTZ	1.413	-0.104
HF/aug-cc-pVQZ	1.412	-0.100
MP2/aug-cc-pVDZ	-2.427	-2.900
MP2/aug-cc-pVTZ	-2.744	-3.313
MP2/aug-cc-pVQZ	-2.790	-3.421
CCSD(T)/aug-cc-pVDZ	-1.832	-2.279
$E_{\text{MP2}(\text{limit})}^b$	-2.823	-3.499
$\Delta\text{CCSD(T)}(\text{limit})^c$	0.658	0.747
$E_{\text{CCSD(T)}(\text{limit})}^d$	-2.165	-2.752
$\Delta\text{ZPE}^e$	0.431	0.366
$D_0$ (calcd) <sup>f</sup>	1.734	2.386
$D_0$ (exptl) <sup>g</sup>	1.4 ± 0.2	2.7 ± 0.1

<sup>a</sup> Energy in kcal/mol. BSSE was corrected by the counterpoise method. Geometries are shown in Figure 5. See text. <sup>b</sup> MP2 interaction energy at the basis set limit.  $E_{\text{MP2}(\text{limit})}$  was estimated using Helgaker's method from the calculated MP2 interaction energies with the aug-cc-pVTZ and aug-cc-pVQZ basis sets. <sup>c</sup> CCSD(T) correction term ( $\Delta\text{CCSD(T)} = E_{\text{CCSD(T)}} - E_{\text{MP2}}$ ) at the basis set limit. See text and the Supporting Information. <sup>d</sup> CCSD(T) interaction energy at the basis set limit.  $E_{\text{CCSD(T)}(\text{limit})} (= E_{\text{MP2}(\text{limit})} + \Delta\text{CCSD(T)}(\text{limit}))$  corresponds to  $-D_e$ . <sup>e</sup> Change of vibrational zero-point energy by formation of cluster. <sup>f</sup> Binding energy of cluster. ( $D_0 = D_e - \Delta\text{ZPE}$ ) <sup>g</sup> This work.

Detailed evaluations of bond functions are shown in the Supporting Information.

The MP2 method overestimates the attraction compared to CCSD(T), which shows that electron correlation beyond MP2 is important. The estimated  $E_{\text{CCSD(T)}(\text{limit})}$  values for the clusters, which correspond to  $-D_e$ , are -2.17 and -2.75 kcal/mol, respectively. Estimated errors of the  $E_{\text{CCSD(T)}(\text{limit})}$  for the clusters are 0.08 and 0.14 kcal/mol, respectively. MP2/cc-pVTZ level optimized geometries were used for the estimation of the  $E_{\text{CCSD(T)}(\text{limit})}$ . The error of  $E_{\text{CCSD(T)}(\text{limit})}$  associated with an inaccuracy of the optimized geometries is very small (probably <0.04 kcal/mol). Errors of the  $E_{\text{CCSD(T)}(\text{limit})}$  for the benzene-ethylene and benzene-acetylene clusters associated with the estimation are 0.04 and 0.10 kcal/mol, respectively. Detailed discussions on the errors of  $E_{\text{CCSD(T)}(\text{limit})}$  are shown in the Supporting Information.

Calculated vibrational zero-point energies (ZPE) for the benzene-ethylene and benzene-acetylene clusters and isolated benzene, ethylene, and acetylene are 95.916, 80.214, 63.199, 32.287, and 16.649 kcal/mol, respectively. Changes of ZPEs by formation of the benzene-ethylene and benzene-acetylene clusters ( $\Delta\text{ZPE}$ ) are 0.431 and 0.366 kcal/mol, respectively. Estimated binding energies for the clusters ( $D_0 = D_e - \Delta\text{ZPE}$ )

**TABLE 2: Electrostatic and Dispersion Energies for CH/ $\pi$  Clusters<sup>a</sup>**

	$E_{\text{total}}^b$	$E_{\text{es}}^c$	$E_{\text{rep}}^d$	$E_{\text{corr}}^e$
benzene-methane <sup>f</sup>	-1.47	-0.19	1.21	-2.50
benzene-ethylene	-2.17	-0.38	1.80	-3.58
benzene-acetylene	-2.75	-1.70	1.60	-2.65

<sup>a</sup> Energy in kcal/mol. Geometries are shown in Figure 5. <sup>b</sup> CCSD(T) interaction energy at the basis set limit. See text. <sup>c</sup> Electrostatic energy. See text. <sup>d</sup> Repulsion energy ( $E_{\text{rep}} = E_{\text{HF}} - E_{\text{es}}$ ).  $E_{\text{HF}}$  is HF/aug-cc-pVQZ interaction energy. See text. <sup>e</sup> Correlation interaction energy ( $= E_{\text{total}} - E_{\text{HF}}$ ).  $E_{\text{corr}}$  is mainly dispersion energy. See text. <sup>f</sup> See ref 20.

are 1.73 and 2.39 kcal/mol, respectively. They are close to the experimental  $D_0$  values ( $1.4 \pm 0.2$  and  $2.7 \pm 0.2$  kcal/mol, respectively). The good agreement between the experimentally determined and theoretical values proves the high quantitative reliability of the present CCSD(T)(limit) level calculations.<sup>42</sup>

**4. Electrostatic and Dispersion Energies.** Electrostatic energies ( $E_{\text{es}}$ ) in the benzene-ethylene and benzene-acetylene clusters are summarized in Table 2.  $E_{\text{total}}$  is the estimated  $E_{\text{CCSD(T)}(\text{limit})}$ .  $E_{\text{corr}}$  is the effect of electron correlation on the calculated total interaction energy, which is the difference between the  $E_{\text{total}}$  and  $E_{\text{HF}}$ . The  $E_{\text{HF}}$  is the calculated HF level interaction energy using the aug-cc-pVQZ basis set. The dispersion interaction is the major contributor to  $E_{\text{corr}}$ .  $E_{\text{rep}} (= E_{\text{HF}} - E_{\text{es}})$  is mainly exchange-repulsion energy, but it also includes some other terms.

The large  $E_{\text{corr}}$  in the benzene-ethylene cluster (-3.58 kcal/mol) shows that dispersion is the major source of the attraction. The electrostatic contribution ( $E_{\text{es}} = -0.38$  kcal/mol) is very small, which shows that the C-H bond of ethylene ( $\text{sp}^2$  C-H bond) is not largely activated. These calculations demonstrate that the interaction between a C-H bond of alkene and  $\pi$ -electrons should be categorized into the typical CH/ $\pi$  interaction. This is consistent with the low-frequency shift of the  $S_1-S_0$  transition of benzene-ethylene, which is seen in Figure 1.

The  $E_{\text{es}}$  in the benzene-acetylene cluster (-1.70 kcal/mol) is considerably larger than those in the benzene clusters with methane and ethylene. Although the  $E_{\text{corr}}$  is still larger (more negative) than the  $E_{\text{es}}$ , both electrostatic and dispersion interactions are important for the attraction in the benzene-acetylene cluster. The large electrostatic contribution shows that the C-H bond of acetylene ( $\text{sp}$  C-H bond) is substantially activated, and the intermolecular interaction is  $\pi$ -hydrogen-bond-like. This is also consistent with the spectroscopic signs in benzene-acetylene; the high-frequency shift of the  $S_1-S_0$  transition and the low-frequency shift of the acetylenic C-H stretch band.<sup>12,18,36-38</sup> A previously reported  $E_{\text{es}}$  value (-2.01 kcal/mol) from a HF/6-311G\*\* calculation is slightly larger than that obtained from the MP2/cc-pVTZ calculation in this work owing to an overestimation of the electrostatic energy by the HF method.<sup>10</sup>

The nature of the "activated" C-H/ $\pi$  interaction in the benzene-acetylene cluster is completely different from that of the "nonactivated" or "typical" C-H/ $\pi$  interaction in the benzene-methane and benzene-ethylene clusters. In the activated C-H/ $\pi$  interaction in the benzene-acetylene cluster, the highly orientation-dependent electrostatic interaction contributes to the attraction substantially. Therefore the C-H/ $\pi$  interaction in the benzene-acetylene cluster would exhibit strong orientation dependence, although the dependence would be smaller than that in conventional hydrogen bonds, where the electrostatic interaction is mainly responsible for the attraction. On the other hand, the electrostatic contribution to the attraction in the "nonactivated" C-H/ $\pi$  interaction in the benzene-methane and

benzene–ethylene clusters is very small, which suggests that the orientation dependence of the interaction energy of “non-activated” C–H/ $\pi$  interactions in these clusters is negligible.

The interaction energy ( $E_{\text{total}}$ ) of the benzene–acetylene cluster (–2.75 kcal/mol) is about twice as large as that of the benzene–methane cluster (–1.47 kcal/mol). The electrostatic interaction in the acetylene cluster (–1.70 kcal/mol) is larger than that in the methane cluster (–0.19 kcal/mol), which is the cause of the larger  $E_{\text{total}}$ . The  $E_{\text{total}}$  of the benzene–ethylene cluster (–2.17 kcal/mol) is also larger than that of the benzene–methane cluster, whereas the electrostatic energies of the two clusters are small (–0.38 and –0.19 kcal/mol, respectively). The  $E_{\text{corr}}$  values of the two clusters (–2.50 and –3.58 kcal/mol, respectively) show that the large dispersion energy in the benzene–ethylene cluster is mainly responsible for the large  $E_{\text{total}}$ .

## Summary

The CH/ $\pi$  interaction energies (the binding energies in the neutral ground state) were determined experimentally and theoretically for the two model cluster systems, benzene–ethylene and benzene–acetylene. Mass-selected, two-color, multiphoton ionization spectroscopy was employed for the experimental determination of the interaction energy of these clusters. Although the interaction energy in benzene–ethylene is slightly enhanced in comparison with that of benzene–methane, more remarkable enhancement of the interaction energy was found for benzene–acetylene, demonstrating the clear activation of the CH/ $\pi$  interaction. The experimentally determined interaction energies agreed well with the theoretical results at the CCSD(T)(limit) level. The calculated electrostatic and dispersion contributions clearly show that the nature of the activated CH/ $\pi$  interaction is significantly different from that of the typical (nonactivated) CH/ $\pi$  interaction. The dispersion interaction is the dominant contributor to the attraction in the typical CH/ $\pi$  interaction in the benzene–methane and benzene–ethylene. On the other hand, the electrostatic interaction is as strong as the dispersion in the activated CH/ $\pi$  interaction in the benzene–acetylene, and the CH/ $\pi$  interaction of alkyne has the  $\pi$ -hydrogen-bond-like nature.

**Acknowledgment.** This work was supported in part by MEXT Japan through projects (Nos. 1600200, 17310057, and 18656009) of the Grant-in-Aid. We thank Tsukuba Advanced Computing Center for the provision of the computational facilities. This work was supported by the Next Generation Super Computing Project, Nanoscience Program, MEXT, Japan.

**Supporting Information Available:** Detailed estimations of the errors in the  $E_{\text{CCSD(T)(limit)}}$  values and effects of the geometry optimization of monomers. These materials are available free of charge via the Internet at <http://pubs.acs.org>.

## References and Notes

- Desiraju, G. R.; Steiner, T. *The Weak Hydrogen Bond*; Oxford University Press: New York, 1999.
- Scheiner, S. *Hydrogen Bonding*; Oxford University Press: New York, 1997.
- Nishio, M.; Hirota, M.; Umezawa, Y. *The CH/ $\pi$  Interaction*; Wiley-VCH: New York, 1998 and references therein.
- Bürgi, T.; Droz, T.; Leutwyler, S. *Chem. Phys. Lett.* **1995**, *246*, 291.
- Braun, J. E.; Mehnert, T. H. Neusser, H. J. *Int. J. Mass Spectrom.* **2000**, *203*, 1.
- Yamakawa, M.; Yamada, I.; Noyori, R. *Angew. Chem., Int. Ed.* **2001**, *40*, 2818.
- Tsuzuki, S.; Honda, K.; Uchimaru, T.; Mikami, M.; Fujii, A. *J. Phys. Chem. A* **2006**, *110*, 10163.
- Jones, M., Jr. *Organic Chemistry*, 2nd ed.; W. W. Norton & Company: New York, 2000.
- Philip, D.; Robinson, J. M. A. *J. Chem. Soc. Perkin Trans. II* **1988**, 1643.
- Tsuzuki, S.; Honda, K.; Uchimaru, T.; Mikami, M.; Tanabe, K. *J. Am. Chem. Soc.* **2000**, *122*, 3746.
- Takahashi, O.; Kohno, Y.; Iwasaki, S.; Saito, K.; Iwaoka, M.; Tomoda, S.; Umezawa, Y.; Tsuboyama, S.; Nishio, M. *Bull. Chem. Soc. Jpn.* **2001**, *74*, 2421.
- Fujii, A.; Morita, S.; Miyazaki, M.; Ebata, T.; Mikami, N. *J. Phys. Chem. A* **2004**, *108*, 2652.
- Voronkov, M. G. *J. Phys. Chem. (U.S.S.R.)* **1947**, *21*, 969.
- McKinnis, A. C. *Ind. Eng. Chem.* **1955**, *47*, 850.
- West, R.; Kraihanzel, C. S. *J. Am. Chem. Soc.* **1961**, *83*, 765.
- Brand, J. C. D.; Eglinton, G.; Tyrrell, J. J. *Chem. Soc.* **1965**, 5914.
- Sundararajan, K.; Viswanathan, K. S.; Kulkarni, A. D.; Gadre, S. R. *J. Mol. Struct.* **2002**, *613*, 209.
- Ramos, C.; Winter, P. R.; Stearns, J. A.; Zwier, T. S. *J. Phys. Chem. A* **2003**, *107*, 10280.
- Morita, S.; Fujii, A.; Mikami, N.; Tsuzuki, S. *J. Phys. Chem. A* **2006**, *110*, 10583.
- Shibasaki, K.; Fujii, A.; Mikami, N.; Tsuzuki, S. *J. Phys. Chem. A* **2006**, *110*, 4397.
- Wiley, W. C.; McLaren, I. H. *Rev. Sci. Instrum.* **1955**, *26*, 1150.
- Chewter, L. A.; Sander, M.; Müller-Dethlefs, K.; Schlag, E. W. *J. Chem. Phys.* **1987**, *86*, 4737.
- Chupka, W. A. *J. Chem. Phys.* **1993**, *98*, 4520.
- Frisch, M. J.; Trucks, G. W.; Schlegel, H. B.; Scuseria, G. E.; Robb, M. A.; Cheeseman, J. R.; Montgomery, J. A., Jr.; Vreven, T.; Kudin, K. N.; Burant, J. C.; Millam, J. M.; Iyengar, S. S.; Tomasi, J.; Barone, V.; Mennucci, B.; Cossi, M.; Scalmani, G.; Rega, N.; Petersson, G. A.; Nakatsuji, H.; Hada, M.; Ehara, M.; Toyota, K.; Fukuda, R.; Hasegawa, J.; Ishida, M.; Nakajima, T.; Honda, Y.; Kitao, O.; Nakai, H.; Klene, M.; Li, X.; Knox, J. E.; Hratchian, H. P.; Cross, J. B.; Bakken, V.; Adamo, C.; Jaramillo, J.; Gomperts, R.; Stratmann, R. E.; Yazyev, O.; Austin, A. J.; Cammi, R.; Pomelli, C.; Ochterski, J. W.; Ayala, P. Y.; Morokuma, K.; Voth, G. A.; Salvador, P.; Dannenberg, J. J.; Zakrzewski, V. G.; Dapprich, S.; Daniels, A. D.; Strain, M. C.; Farkas, O.; Malick, D. K.; Rabuck, A. D.; Raghavachari, K.; Foresman, J. B.; Ortiz, J. V.; Cui, Q.; Baboul, A. G.; Clifford, S.; Cioslowski, J.; Stefanov, B. B.; Liu, G.; Liashenko, A.; Piskorz, P.; Komaromi, I.; Martin, R. L.; Fox, D. J.; Keith, T.; Al-Laham, M. A.; Peng, C. Y.; Nanayakkara, A.; Challacombe, M.; Gill, P. M. W.; Johnson, B.; Chen, W.; Wong, M. W.; Gonzalez, C.; Pople, J. A. *Gaussian 03, Revision C.02*; Gaussian, Inc.: Wallingford, CT, 2004.
- Møller, C.; Plesset, M. S. *Phys. Rev.* **1934**, *46*, 618.
- Head-Gordon, M.; Pople, J. A.; Frisch, M. J. *Chem. Phys. Lett.* **1988**, *153*, 503.
- Pople, J. A.; Head-Gordon, M.; Raghavachari, K. *J. Chem. Phys.* **1987**, *87*, 5968.
- Ransil, B. J. *J. Chem. Phys.* **1961**, *34*, 2109.
- Boys, S. F.; Bernardi, F. *Mol. Phys.* **1970**, *19*, 553.
- Helgaker, T.; Klopper, W.; Koch, H.; Noga, J. *J. Chem. Phys.* **1997**, *106*, 9639.
- Tao, F.-M.; Pan, Y.-K. *J. Chem. Phys.* **1992**, *97*, 4989.
- Stone, A. J.; Dullweber, A.; Hodges, M. P.; Popelier, P. L. A.; Wales, D. J. *Orient: a program for studying interactions between molecules*, version 3.2; University of Cambridge, 1995.
- Stone, A. J. *The theory of intermolecular forces*; Clarendon Press: Oxford, 1996.
- Stone, A. J.; Alderton, M. *Mol. Phys.* **1985**, *56*, 1047.
- Stone, A. J. *J. Chem. Theory Comput.* **2005**, *1*, 1128.
- Carrasquillo, E.; Zwier, T. S.; Levy, D. H. *J. Chem. Phys.* **1985**, *83*, 4990.
- Shelly, M. Y.; Dai, H.-L.; Troxler, T. J. *Chem. Phys.* **1999**, *110*, 9081.
- Sampson, R. K.; Bellm, S. M.; Gascooke, J. R.; Lawrence, W. D. *Chem. Phys. Lett.* **2003**, *372*, 307.
- Leutwyler, S. *Chem. Phys. Lett.* **1984**, *107*, 284.
- Gonohe, N.; Suzuki, N.; Abe, H.; Mikami, N.; Ito, M. *Chem. Phys. Lett.* **1983**, *94*, 549.
- Gotch, A.; Zwier, T. S. *J. Chem. Phys.* **1992**, *96*, 3388.
- The expected errors of estimated  $E_{\text{CCSD(T)(limit)}}$  in the benzene clusters with ethylene and acetylene are 0.08 and 0.14 kcal/mol, respectively. The errors of  $\Delta ZPE$  will be less than 0.05 kcal/mol (10 % of  $\Delta ZPE$ ). Therefore, errors of the calculated  $D_0$  for the clusters are 0.13 and 0.19 kcal/mol, respectively. Errors of experimental  $D_0$  caused by the uncertainties in the threshold determination and the filed ionization correction term will be 0.2 kcal/mol. These errors would be the sources of remaining 0.3 kcal/mol discrepancy between the theoretical and experimental  $D_0$  values. Details of the evaluation of the errors are described in the Supporting Information.